RSC Advances

ROYAL SOCIETY OF CHEMISTRY

www.rsc.org/advances

Co-delivery of siRNA and doxorubicin to cancer cells from additively manufactured implants

Muwan Chen[1,2,#], Morten Ø. Andersen[1,3,4,#,*], Philipp Dillschneider[1,3], Chi-Chih Chang[1,3], Shan Gao[1,3], Dang Q. S. Le[2], Chuanxu Yang [1,3], San Hein[1,3], Cody Bünger[2], Jørgen Kjems[1,3]

[1]Interdisciplinary Nanoscience Center, Aarhus University, Aarhus, Denmark.

[2]Orthopaedic Research Laboratory, Aarhus University Hospital, Aarhus, Denmark.

[3]Department of Molecular Biology and Genetics, Aarhus University, Aarhus, Denmark.

[4]The Maersk Mc-Kinney Moller Institute, University of Southern Denmark, Odense, Denmark.

# These authors contributed equally to this work.

*Corresponding author: Email: moan@mmmi.sdu.dk, Telephone: +45 21261877

Short Running Title: Scaffold delivery of siRNA and doxorubicin

Abstract

Tumors in load bearing bone tissue are a major clinical problem, in part because surgical resection invokes a dilemma whether to resect aggressively, risking mechanical failure, or to resect conservatively, risking cancer recurrence due to residual malignant cells. A chemo-functionalized implant, capable of physically supporting the void while killing residual cancer cells, would be an attractive solution. Here we describe a novel additively manufactured implant that can be functionalized with chitosan/siRNA nanoparticles. These induce long term gene silencing in adjacent cancer cells without showing toxicity to normal cells. When scaffolds are functionalized with siRNA/chitosan nanoparticles and doxorubicin in combination, their effects synergized leading to cancer cell death. This technology may be used to target resistance genes by RNA interference and thereby re-sensitizing the cancer cells to co-delivered chemotherapy.

Keywords: Scaffold, Controlled Release, siRNA, Doxorubicin, Cancer, Co-delivery

Introduction

Primary tumors and metastatic secondary tumors to the spine are major clinical problems in oncology and treatment is primarily palliative [1]. Treatment either consists of radiation therapy or surgical removal of the tumor. In the case of surgery, extra complications from radical intervention like complete spondylectomy must be weighed against increased recurrence associated with conservative resection due to residual tumor tissue [2]. As the surgical void is commonly filled with a scaffold to provide mechanical support several studies have investigated the possibility of releasing chemotherapy from such scaffolds to kill the remaining cancer cells [3-7].

A wide variety of drug may be released from scaffolds[8, 9]. We have previously shown that it is possible to develop a void filling scaffold capable of slowly releasing the chemotherapeutic doxorubicin while also supporting the formation of new bone *in vitro* and *in vivo* [10, 11]. These scaffolds were made from anionic polycaprolactone and were coated with cationic chitosan and an anionic montmorillonite clay layer capable of controlled doxorubicin release. Importantly, these scaffolds were created using computer controlled fused deposition modeling, a type of additive manufacturing also known as 3D printing. This technique enables the synthesis of tailor made scaffolds that can be made to fit e.g. individual computed tomography scanning data [12].

For all chemotherapies there is always a risk that individual cancer cells may possess or develop resistance by expressing anti-apoptotic genes such as the B-Cell Lymphoma-2 (BCL2) family (e.g. BCL2, BCLxL/BCL2L1 and BCLw/BCL2L2) [13] or drug export channels such as the multidrug resistance family (e.g. MDR1) [14]. Previous results have shown that cancer cells often can be re-sensitized by inhibiting these genes using small molecule inhibitors [15] or small interfering RNAs (siRNAs) [16]. In this study we investigate the co-delivery of chemotherapy and siRNA from scaffolds. RNA interference (RNAi) therapeutics, such as siRNA and microRNA (miRNA) mimics, are double stranded RNA molecules which deliver a guide strand to the cytoplasmic RNA-induced

silencing complex (RISC). This strand then guides RISC to specific mRNAs by base pairing leading to subsequent silencing of the mRNA by enhanced degradation or inhibition of translation [17]. Active RNAi molecules can be used as chemotherapeutics themselves [18, 19] but have also been co-delivered with chemotherapy in several studies [20, 21]. Many of these studies have investigated the intra venous delivery route but systemic RNAi therapy is hampered by many barriers such as serum nuclease induced degradation, kidney secretion, sequestration by the mononuclear phagocyte system and poor extravasation and delivery to the target site [22]. Even if these barriers may potentially be overcome, unspecific systemic delivery may damage healthy tissues as the genes responsible for chemotherapy resistance often play vital roles in cell homeostasis. The BCL2 family, for example, plays a key role in promoting neuroprotection [23].

Local release of siRNA from implants has previously been used to address areas as different as bone resorption [24], fibrosis [25, 26], angiogenesis [27], neurite outgrowth [28], insufficient stem cell proliferation [29] and stem cell differentiation [30]. By delivering siRNA from a scaffold, the siRNA activity is localized and thus less damage to remote susceptible tissue. Even though local delivery circumvents many of the *in vivo* barriers to systemic siRNA delivery [24, 26], the siRNA still needs to be delivered to the cytoplasm of the cancer cells by a transfection agent. Several agents have previously been developed [31, 32]. We have, for example, shown that nanoparticles formed through electrostatically driven self-assembly of the cationic carbohydrate polymer chitosan and anionic siRNA can efficiently transfect cancer cells and induce gene silencing *in vitro* and *in vivo* [33]. Nanoparticles composed of chitosan and plasmids that encode tumor suppressors have also been combined with doxorubicin to induce cell death in hepatocellular carcinoma cells, demonstrating the potential of combining nucleic acid therapy with conventional chemotherapy [34].

We hypothesize that siRNA may be released locally from a scaffold and induce gene silencing in adjacent cancer cells. If targeted towards resistance genes and co-released together with anti-cancer

drugs such a system could potentially overcome drug resistance and prevent the recurrence of cancer at the resection/implantation site. In this study we develop such a dual-delivery scaffold. We demonstrate that a novel 3D printed scaffold coated with chitosan, montmorillonite clay and tricalciumphosphate can be further functionalized with doxorubicin and lyophilized chitosan/siRNA nanoparticles. We show that the siRNA is released slowly from the scaffolds and that chitosan/siRNA nanoparticles can induce sequence specific gene silencing in lung cancer and glioma cells. The gene silencing sustained for at least 7 days and could be induced in a co-culture of healthy cells and cancer cells. We also find that co-delivering chitosan/siRNA nanoparticles with doxorubicin increases chemotherapy induced toxicity to the cancer cells.

Experimental Section

Materials

The nanoclay was Cloisite Na+, Lot: 07F28GDX-008 (Southern Clay Products, Inc, Moosburg, Germany). The chitosan for scaffold fabrication was performed with Chitopharm M with 75%–85% degree of deacetylation (Cognis, Florham Park, NJ). Polycaprolactone (MW = 50 kDa) was obtained from Perstorp (Cheshire, UK). The β-TCP nanocrystals were from Berkeley Advanced Biomaterials, Inc, Berkeley, CA (Lot: TCPCH01). Dexamethasone, L-ascorbic acid and 1α, 25-dihydroxyvitamin D3, Naphtol-AS-TR phosphate and Fast red were purchased from (Sigma, US), β-glycerophospate was from (Calbiochem, US) and medium components were obtained from (Gibco, US).

Chitosan, for use as transfection agent was acquired from Novamatrix, Norway. Before use it was further deacetylated and characterized as described previously [35]. The chitosan applied in this study was 98% de-acetylated with a molecular weight of 250 kDa. GFP-targeted (siGFP), GFP-Mismatched (siMM), BCLw targeted (siBCLw) and Cy3-labeled GFP-targeted siRNA were

synthesized by Ribotask (Denmark). The sequences were: EGFP targeted siRNA (sense strand: 5′-GACGUAAACGGCCACAAGUUC-3′, antisense strand: 3′-GCUGCAUUUGCCGGUGUUCA-5′), EGFP mismatch siRNA (sense strand: 5′-GACGUUAGACUGACAAGUUC-3′, antisense strand: 3′-CGCUGAAUCUGACCUGUGGUUCA-5′) and BCLw targeted siRNA (sense strand: 5′-CCCAGGUCUCCGAUGAACUdTdT-3′, antisense strand: 3′-dTdTGGGUCCAGAGGCUACUUGA-5′).

Cell Lines

DSRED2-expressing adipose-derived murine mesenchymal stem cells (mMSCs) from C57BL/6 mice were acquired from B-Bridge International and primary human bone marrow-derived mesenchymal stem cells (hMSCs) were obtained from ATCC. Both were cultured in αMEM containing 10% FBS and 1% P/S before using them at passage 10. The H1299 cells were a gift from Anne Chauchereau whereas the GFP-expressing HeLa and U251 cells were prepared in-house. Green fluorescent protein expressing (GFP^+) or wild type (GFP^-) H1299, HeLa and U251 cells were cultured in RPMI containing 10% FBS and 1% P/S. The medium wherein the GFP^+ H1299 cells were grown also contained 0.5% G418. The cells were passaged every 3-4 days.

Implant Production

Implants were produced as previously described [10]. Briefly, 3D PCL printed scaffolds (d = 4 mm, h = 2 mm) were immersion coated with 1% w/v chitosan in 1% v/v acetic acid solution, containing montmorillonite clay (weight ratio to chitosan is 1:10), and tricalciumphosphate (weight ratio to chitosan is 1:20). Scaffolds were freeze-dried and then neutralized in 70% Ethanol containing 0.4 M NaOH and then rinsed in PBS three times and freeze-dried again. A photograph of the used scaffold is shown in Figure 1b.

Drug Coating of Implants

Chitosan/siRNA nanoparticles were made by slowly adding 20 µL 100 µM siRNA to 1mL 720 µg/mL chitosan in 0.3 M NaAc buffer (pH 5.5) while stirring vigorously. After 1 hour of stirring 200 µL of sucrose solution (60 mg sucrose in 100 mL water) was added and 25 µL of the resulting solution were added to the scaffolds giving a theoretical loading of 41 pmol siRNA per scaffold. The chitosan/siRNA nanoparticles have previously been extensively characterized using atomic force microscopy, particle tracking, dynamic light scattering and zeta potential measurements and have been found to be spherical with a hydrodynamic radius between 100 nm and 200 nm with strongly positive zeta potential > 40 mV [33, 35, 36, 37]. Five minutes after addition of the nanoparticles the implants were frozen on dry ice and freeze dried until dry at -20°C and 12 mT.

Where doxorubicin was used, 2.5 µL 1 mg/mL was added to the 25 µL transfection mix immediately before addition to the scaffolds, 25 µL of this mix was then used to coat each scaffold giving a maximum loading of 0.909 µg of doxorubicin per scaffold.

SEM

Dehydrated scaffolds, with or without chitosan/siRNA nanoparticle functionalization, were placed on aluminum SEM stubs using double-sided tape and visualized using a NovaSEM (FEI, OR). The following settings were used: Low vacuum detector, 60 Pa H_2O, spot size: 3, voltage: 5 kV, working distance approximately 5 mm. Representative pictures are shown with scale bars.

Release Experiment

Non-functionalized and scaffolds functionalized with chitosan nanoparticles containing cy3-labeled siRNA were placed in the inner wells on a 96 well plate where all outer wells were filled with PBS

to minimize evaporation. Three hundred microliters of PBS were then added to each scaffold and the plate was stored sealed at 37°C. After 1, 3, 24, 48, 72, 120, and 168 hours the PBS was removed, stored in a 96 well plate at -20°C and replaced by 300 µL PBS. At the end of the assay, the frozen plate was freeze-dried and added 100 µl PBS for release measurement at ex/em: 540nm/580nm. Scaffolds after the release study were observed under a fluorescence microscope (Olympus IX71 equipped with Cy3 filter).

Cell Culture & Seeding

Approximately $1x10^5$ cells (for mono-culture experiments) or $5x10^4$ cells of each cell type (for co-culture experiments) were seeded in 12-well plates in 1 mL of complete medium. After 24 hours the medium was replaced with 500 µL complete medium and scaffolds were added (Figure 1c). Medium was changed on the second day and the fourth day after scaffolds were added. At the indicated days cells were harvested for flow cytometry or were analyzed for viability. Viability studies were performed in 96-well plates with 10 times lower volumes.

Viability

At the indicated day the medium was aspirated, the scaffold removed and the wells washed with PBS before addition of 100 µL MTT (0.5 mg/mL in MEM medium) to each well. After 30 min incubation at 37°C the MTT solution was removed and the MTT solubilized in 100 µL DMSO. Absorbance was measured at 570 nm using a µQuant plate spectrophotometer (BioTek). Absorbance from empty wells was subtracted from the resulting values.

Flow Cytometry

After the indicated number of days the cells were washed with PBS and harvested with 500 µL trypsin which was afterwards deactivated with 500 µL complete medium. The cell suspension was centrifuged 5 min at 1500 RPM, the pellet resuspended in 1% paraformaldehyde and stored at 4^0C until flow cytometry was performed on a Gallios flow cytometer (Beckman Coulter, Inc.). The median GFP fluorescence of the cell population, gated using forward- and side-scatter, was used as a read out. In the H1299/mMSC co-culture experiment, the H1299 cell population was isolated by deselecting red fluorescent cells (The $DSRED^+$ mMSCs).

Alkaline Phosphatase

hMSCs were seeded at 10 000/cm^2 in a 24 well. The next day, scaffolds were placed into the wells and half of the wells were induced with osteogenic media containing 10 nM Dexamethasone, 0.2 mM L-ascorbic acid, 10 mM β-glycerophospate and 10 mM 1α, 25-dihydroxyvitamin D_3. Differentiation media was changed every 2-3 days. Staining was performed at day 7 of osteogenesis. The cells were washed in PBS and fixed with acetone/10 mM citrate buffer (pH 4.2) (1.5:1, v:v) for 5 minutes at room temperature. Staining solutions 0.2 mg /ml Naphtol-AS-TR phosphate(Sigma) in ddH2O and 0.83 mg/ml Fast red (Sigma) in 0.1 M Tris buffer (pH9.0) were mixed (1:1.2, v:v) prior to staining. Cells were stained for 1 hour at room temperature. Excess stain was washed off with deionized water. Photomicroscopy was used to analyze the staining with the Olympus IX71Microscope.

Statistics

Statistical analysis was performed in R (version 3.0.2). One-way (all figures) and two-way (Figure 7) ANOVA was used to test the difference within groups and TukeyHSD was used to determine which groups had significantly different mean. P-values were taken to be significant if they were

below an alpha level of 0.05. In certain stated cases Welch's t-tests were performed. All figures show averages with standard deviation displayed as error bars; in general the average and standard deviations are normalized to a control group to ease visual comparison. The number of samples (n) is given, as is the p-value for the ANOVA test.

Results

The clinical problem and our approach to address it are illustrated in Figure 1.

Scaffolds with and without a chitosan/siRNA nanoparticle functionalization were produced and the morphology was investigated using SEM at 200x and 1000x magnification (Figure 2). The PCL fibers of the non-functionalized scaffolds (Figure 2a-b) contained a thin coat, presumably consisting of chitosan, with extensive micro- and nano featuring likely composed of montmorrilonite clay and tricalciumphosphate. The fibers visible in the chitosan/siRNA nanoparticle functionalized scaffold (Figure 2c-d) were covered with a thick smooth layer that obscured the features observed in the non-functionalized scaffolds. The functionalization likely appears smooth due to the lyoprotectant matrix of sucrose that surrounds the particles.

To test the chitosan/siRNA coat, we produced scaffolds functionalized with chitosan nanoparticles that were formulated with GFP targeted (siGFP) or mismatched siRNA (siMM). Each type of scaffold was added to wells containing three different GFP-expressing human cancer cell lines H1299 (non-small cell lung carcinoma, NSCLC), HeLa (cervical carcinoma) and U251 (glioma) for two days before harvesting and analyzing by flow cytometry (Figure 3). The chitosan/siRNA functionalized scaffold induced an unspecific increase in fluorescence in all cell types (likely due to auto fluorescence of chitosan) but they also induced sequence specific silencing of GFP in the H1299 and U251 cells when comparing siGFP to siMM (71% and 32% reduction, $p < 0.0002$ and $p = 0.01$, respectively). Since the NSCLC cells (H1299) are efficiently transfected and a relevant

target given the high tendency of NSCLC to metastasize to the bone [38], we decided to further investigate the effect of the functionalized scaffolds on these cells.

To further evaluate the extent and duration of knockdown we coated scaffolds with siGFP and siMM and transferred them to wells containing pre-seeded GFP-expressing H1299 cells. At day 3 and 7 after exposure to the scaffold, the degree of GFP-silencing was evaluated using flow cytometry (Figure 4a). After 3 days a large fraction of the cells showed a reduction in GFP fluorescence when cultured in the presence of siGFP functionalized scaffolds compared to cells grown with siMM functionalized control scaffolds (Figure 4a). At day 3, the median GFP fluorescence was also significantly reduced in cells cultured together with siGFP functionalized scaffolds compared to cells grown with no scaffold, non-functionalized scaffolds or siMM functionalized scaffolds (59%, 40% and 61% reduction, $p < 1E-7$, $p < 0.0003$ and $p < 1E-7$, respectively; Figure 4b). At day 7, the median GFP fluorescence was significantly reduced in cells cultured together with siGFP functionalized scaffolds as compared to cells grown without a scaffold or with siMM functionalized scaffold (53% and 65% reduction, $p < 0.01$ and $p < 5E-5$, respectively). There was no significant difference in silencing between day 3 and 7 (t-test of the siGFP/siMM ratio for day 3 and 7, $p = 0.1$; Figure 4b).

The adjacent tissue to the surgical void, which is exposed to siRNAs, will contain both cancer cells and healthy cells. It is thus important that the siRNA cause silencing in the cancer cells also in the presence of normal cells. To evaluate delivery of siRNA to cancer cells in the presence of another cell type $5x10^4$ H1299 (GFP^-) cells were seeded alone or with $5x10^4$ primary mouse mesenchymal stem cells (mMSC) ($DSRED^+$, p11) in 12-well plates with 1:1 (V/V) RPMI and MEM medium supplemented with 10% FBS and 1% P/S. After 24 hours scaffolds were added and after additional three days of incubation cells were harvested and investigated by flow cytometry (Figure 5). The H1299 cells grew more rapidly than the mMSCs but both cell types were present in significant

numbers at the time of harvesting. The expression of GFP was clearly reduced in the H1299 cell population exposed to scaffolds functionalized with siGFP compared to siMM functionalization (51% and 47% reduction, p = 1E-7 and p = 9E-5, respectively) and to a similar extent under both mono- and co-cultured conditions (t-test of the siGFP/siMM ratio for mono- and co-culture, p = 0.8) indicating that the presence of mMSCs did not interfere with the silencing efficiency.

To investigate whether the implant itself or the chitosan/siRNA nanoparticle coating is toxic to cancer- or healthy cells we cultured H1299 and mMSCs separately in the presence of scaffolds for 3 days followed by a viability test using a MTT assay (Figure 6). Only the H1299 cancer cells were slightly less viable in the presence of the chitosan/siRNA nanoparticle functionalized scaffolds as compared to non-functionalized scaffolds (17% reduction, p = 0.006).

Several studies have indicated that siRNA knock down of certain genes can act synergistically with chemotherapy to induce cytotoxicity. To test this in our system we functionalized scaffolds with different combinations of doxorubicin and chitosan/siRNA nanoparticles. As a potentially functional siRNA target BCLw (BCL2L2) was chosen. BCLw is a BCL2 family protein known to have anti-apoptotic function in H1299 cells and being the target of a pro-apoptotic miRNA in NSCLC [39]. To better observe the siRNA-mediated effect we applied a very low concentration of doxorubicin (0.909 μg per scaffold) which by itself does not induce toxicity. After 3 days of incubation the effect of the combined treatment on the viability of the H1299 cells was determined using a MTT based viability assay (Figure 7). To ensure doxorubicin did not interfere with the spectrophotometric measurements the wells were washed before the MTT assay. Coating of scaffolds with doxorubicin alone did not alter viability (p = 0.8). Also, the BCLw targeted siRNA did not appear to have a sequence specific effect on viability when compared to the mismatched siRNA, with or without doxorubicin (p = 0.6 and p = 0.8, respectively). However, the chitosan/siRNA nanoparticles induced sequence independent effects when compared to the non-

coated control group (as determined by two-way ANOVA). When used alone, they appeared to raise viability compared to the non-coated control group (32% increase, $p = 0.0001$). In contrast, when used in conjunction with doxorubicin, they reduced viability compared to both the non-functionalized control group, the doxorubicin only group and the chitosan/siRNA only group (28%, 21% and 45% reduction, $p = 0.0007$, $p = 0.02$ and $p < 1E-7$, respectively). These results are also indicated in microscopy pictures taken of the cells immediately prior to conducting the MTT assay, these images show fewer cells in the chitosan/siRNA + doxorubicin group compared to the control groups (Supplementary Figure S1).

In order to investigate the release rates of the chitosan/siRNA nanoparticles, chitosan nanoparticles with Cy3-labeled siRNA were loaded onto scaffolds and subsequently incubated at 37 °C in 300 µL PBS. Sink conditions were used as a 100% release would give a calculated siRNA concentration of 5.5 µM siRNA in the solution. Fluorescence intensity was measured for samples collected from various time points and the background signal from the blank wells was subtracted. The accumulative release profiles were calculated based on concentrations obtained (Figure 8). A biphasic release profile was observed with an initial burst release of 15 % of the maximum theoretical siRNA loading at the first time point (1 hour) followed by a sustained slow release, reaching 24 % accumulated siRNA release at day 7. To investigate what happens to the remaining siRNA, we analyzed the scaffolds with fluorescence microscopy after the one-week release study. We observed a substantial amount of Cy3-labeled chitosan/siRNA left on the scaffolds (Figure 8d), compared to the fluorescence background from scaffold alone and scaffold loaded with non-labeled siRNA (Figure 8b and 8c, respectively) suggesting that a considerable fraction of the siRNA remain associated with the scaffold after one week.

Since the scaffolds are supposed to support bone regeneration to fill the void after the tumor elimination we investigated whether hMSCs could initiate osteogenic differentiation in the presence

of the scaffolds with and without chitosan/siRNA nanoparticles and doxorubicin. hMSCs were seeded, scaffolds added and after 24 h osteogenesis was induced by adding osteogenic media in half of the wells. After 7 days, cells were stained for alkaline phosphatase, which is a marker of early osteogenic differentiation (Supplementary Figure S2). Osteogenesis was induced in all sample groups as indicated by positive staining when incubated with osteogenic medium compared to incubation with maintenance medium.

Discussion

Chemotherapy resistance in primary and metastatic bone tumors is a major clinical problem that could be addressed using siRNA targeted against the resistance genes. Towards this aim, we describe a 3D printed polycaprolactone scaffold for void filling after bone tumor resection. We then used the established layer-by-layer implant coating technique [40-44] to coat the anionic scaffold with cationic chitosan and anionic montmorillonite before functionalizing it with a layer of cationic chitosan/siRNA nanoparticles embedded in a sucrose matrix. After freeze drying and when placed in aqueous medium, the nanoparticles were released to the scaffold surroundings where they induced gene silencing (Figure 3-5). That chitosan/siRNA particles can retain functionality even after lyophilization with sucrose, confirming previous results [28, 35].

The scaffolds coated with chitosan/siRNA nanoparticles displayed a small burst release followed by a prolonged phase with slower release (Figure 8). When chitosan/siRNA nanoparticles are added to the scaffolds before lyophilization, we expect that the majority of the nanoparticles will adhere to the scaffold walls driven by ionic interactions between the positively charged chitosan and the negatively charged montmorillonite that appear to be exposed on the scaffold surface in the SEM pictures (Figure 2). Other forces such as hydrogen bonding and van der Waals forces also are likely to play a role [45]. The burst release of a minor portion of the siRNA is probably driven by the

dissolution of the sucrose matrix and simultaneous release of particles that did not adhere to the scaffold. In our study the binding agent (montmorillonite) is thus a dual-functional layer capable of storing and controllably releasing doxorubicin[10] in addition to binding the chitosan/siRNA nanoparticles. Other dual release scaffolds have previously been developed for co-delivering e.g. antimicrobial silver and osteogenic growth factors [46, 47] but to our knowledge not for co-delivering siRNA with chemotherapy.

In our toxicity studies we find that the chitosan/siRNA nanoparticles synergize with a low concentration of doxorubicin to induce toxicity in the lung cancer cells in a siRNA sequence independent manner. It is known that chitosan oligosaccharides [48] and chitosan nanoparticles formulated with mismatched siRNA [49] or with tripolyphosphate [50] can inhibit cancer. One study [51], even found that chitosan nanoparticles induce greater toxicity to cancer cells than free chitosan. The mechanism seems to be a combination of cellular and mitochondrial membrane destabilization, induction of apoptosis and necrosis as well as inhibition of angiogenesis and activation of the immune system [52]. However, the present study uses a lower concentration of chitosan than these studies and we observed little effect on viability from the chitosan/siRNA nanoparticles alone. We speculate that the synergistic effect observed on cell viability, when chitosan nanoparticles are used together with a low concentration of doxorubicin, occurs because chitosan increases the uptake of doxorubicin through destabilization of the cellular membrane and/or because the combination of treatments pushes the cells into apoptosis or necrosis. This synergistic effect may allow lower concentrations of doxorubicin to be used in the final application.

There are only a limited number of other studies that have investigated scaffold mediated delivery of siRNA in relation to cancer therapy. In one study, metastasis promoting Snail-1 was downregulated in fibroblasts seeded in an atelocollagen sponge functionalized with polyamidoamine/siRNA complexes [53]. In another study, chitosan/siRNA nanoparticles encapsulated

in electrospun PLGA fibers were able to silence GFP in H1299 cells seeded onto the fibers [54]. A different study investigated the delivery of a plasmid encoding siRNAs encapsulated into electrospun PCL fibers [55]. When the siRNA was targeted against Cdk-2, a key cell cycle gene, cell death was induced in breast cancer cells seeded onto the fibers. While demonstrating the potential of scaffold based siRNA delivery for cancer applications, these studies did not investigate the delivery of siRNA to cells not residing directly on the scaffold. The present proof of concept paper extends these previous studies by demonstrating that it is possible to functionalize a 3D printed void filling scaffold to co-release functional siRNA and doxorubicin to surrounding cancer cells. The next step will be to test whether it can kill chemotherapy resistant cell lines *in vitro* and *in vivo* when doxorubicin is combined with siRNA targeted against the resistance genes.

Conclusion

We have demonstrated that additively manufactured scaffolds can be functionalized with chitosan/siRNA nanoparticles and that these can be released and induce gene silencing in adjacent cancer cells. We also show that silencing is unaffected by the presence of normal cells and that the formulation in itself is non-toxic in normal cells. Furthermore, when chitosan nanoparticles are combined with doxorubicin a synergistic reduction in cancer cell viability is observed. Co-delivery of siRNA/chitosan and doxorubicin from scaffolds may thus have value in the reduction of cancer recurrence after bone tumor resection.

Acknowledgements

The authors would like to thank Claus Bus and Rita Rosendahl Hansen for valuable technical assistance. This study is supported by grants from the Danish Strategic Research Council (Individualized Musculoskeletal Repair Network, Jr. nr. 09-063120), and Lundbeck Foundation

Nanomedicine Center for Individualized Management of Tissue Damage and Regeneration (LUNA).

References

1. Dunning, E. C.; Butler, J. S.; Morris, S. *World J Orthop* **2012,** 3, (8), 114-21.
2. Cloyd, J. M.; Acosta, F. L., Jr.; Polley, M. Y.; Ames, C. P. *Neurosurgery* **2010,** 67, (2), 435-44; discussion 444-5.
3. DeFail, A. J.; Edington, H. D.; Matthews, S.; Lee, W. C. C.; Marra, K. G. *J Biomed Mater Res A* **2006,** 79a, (4), 954-962.
4. Froschle, G. W.; Mahlitz, J.; Langendorff, H. U.; Achilles, E.; Pollock, J.; Jungbluth, K. H. *Anticancer Res* **1997,** 17, (2A), 995-1002.
5. Wadee, A.; Pillay, V.; Choonara, Y. E.; du Toit, L. C.; Penny, C.; Ndesendo, V. M.; Kumar, P.; Murphy, C. S. *Expert Opin Drug Deliv* **2011,** 8, (10), 1323-40.
6. Xie, J.; Wang, C. H. *Pharm Res* **2006,** 23, (8), 1817-26.
7. Yohe, S. T.; Herrera, V. L. M.; Colson, Y. L.; Grinstaff, M. W. *Journal of Controlled Release* **2012,** 162, (1), 92-101.
8. Krebs, M. D.; Alsberg, E. *Chemistry* **2011**, 17, (11), 3054-62

9. Wu, J.; Zhao, X.; Wu, D.; Chu C. C. *J. Mater. Chem. B* **2014**, 2, 6660-6668

10. Chen, M.; Le, D. Q.; Hein, S.; Li, P.; Nygaard, J. V.; Kassem, M.; Kjems, J.; Besenbacher, F.; Bunger, C. *Int J Nanomedicine* **2012,** 7, 4285-97.
11. Sun, M.; Wang, M.; Chen, M.; Dagnaes-Hansen, F.; Le, D. Q.; Baatrup, A.; Horsman, M. R.; Kjems, J.; Bunger, C. E. *Acta Biomater* **2015,** 18, 21-9.
12. Andersen, M. O.; Le, D. Q. S.; Chen, M. W.; Nygaard, J. V.; Kassem, M.; Bunger, C.; Kjems, J. *Adv Funct Mater* **2013,** 23, (45), 5599-5607.
13. Kim, R.; Emi, M.; Tanabe, K.; Toge, T. *Cancer* **2004,** 101, (11), 2491-2502.
14. Perez-Tomas, R. *Curr Med Chem* **2006,** 13, (16), 1859-76.
15. Oltersdorf, T.; Elmore, S. W.; Shoemaker, A. R.; Armstrong, R. C.; Augeri, D. J.; Belli, B. A.; Bruncko, M.; Deckwerth, T. L.; Dinges, J.; Hajduk, P. J.; Joseph, M. K.; Kitada, S.; Korsmeyer, S. J.; Kunzer, A. R.; Letai, A.; Li, C.; Mitten, M. J.; Nettesheim, D. G.; Ng, S.; Nimmer, P. M.; O'Connor, J. M.; Oleksijew, A.; Petros, A. M.; Reed, J. C.; Shen, W.; Tahir, S. K.; Thompson, C. B.; Tomaselli, K. J.; Wang, B.; Wendt, M. D.; Zhang, H.; Fesik, S. W.; Rosenberg, S. H. *Nature* **2005,** 435, (7042), 677-81.
16. Lo, Y. L.; Liu, Y.; Tsai, J. C. *Biomed Pharmacother* **2013,** 67, (4), 261-267.
17. Carthew, R. W.; Sontheimer, E. J. *Cell* **2009,** 136, (4), 642-55.
18. Pai, S. I.; Lin, Y. Y.; Macaes, B.; Meneshian, A.; Hung, C. F.; Wu, T. C. *Gene Ther* **2006,** 13, (6), 464-77.
19. Salva, E.; Turan, S. O.; Kabasakal, L.; Alan, S.; Ozkan, N.; Eren, F.; Akbuga, J. *J Pharm Sci* **2014,** 103, (3), 785-95.
20. Tsouris, V.; Joo, M. K.; Kim, S. H.; Kwon, I. C.; Won, Y. Y. *Biotechnol Adv* **2014,** 32, (5), 1037-1050.
21. Wei, W.; Lv, P. P.; Chen, X. M.; Yue, Z. G.; Fu, Q.; Liu, S. Y.; Yue, H.; Ma, G. H. *Biomaterials* **2013,** 34, (15), 3912-23.

22. Whitehead, K. A.; Langer, R.; Anderson, D. G. *Nat Rev Drug Discov* **2009,** 8, (2), 129-38.
23. Graham, S. H.; Chen, J.; Clark, R. S. *J Neurotrauma* **2000,** 17, (10), 831-41.
24. Wang, Y. W.; Tran, K. K.; Shen, H.; Grainger, D. W. *Biomaterials* **2012,** 33, (33), 8540-8547.
25. Rujitanaroj, P. O.; Jao, B.; Yang, J.; Wang, F.; Anderson, J. M.; Wang, J.; Chew, S. Y. *Acta Biomater* **2013,** 9, (1), 4513-4524.
26. Takahashi, H.; Wang, Y.; Grainger, D. W. *J Control Release* **2010,** 147, (3), 400-7.
27. Nelson, C. E.; Kim, A. J.; Adolph, E. J.; Gupta, M. K.; Yu, F.; Hocking, K. M.; Davidson, J. M.; Guelcher, S. A.; Duvall, C. L. *Adv Mater* **2014,** 26, (4), 607-14, 506.
28. Mittnacht, U.; Hartmann, H.; Hein, S.; Oliveira, H.; Dong, M.; Pego, A. P.; Kjems, J.; Howard, K. A.; Schlosshauer, B. *Nano Lett* **2010,** 10, (10), 3933-9.
29. Plasilova, M.; Schonmeyr, B.; Fernandez, J.; Clavin, N.; Soares, M.; Mehrara, B. J. *Plast Reconstr Surg* **2009,** 123, (2 Suppl), 149S-57S.
30. Andersen, M. O.; Nygaard, J. V.; Burns, J. S.; Raarup, M. K.; Nyengaard, J. R.; Bunger, C.; Besenbacher, F.; Howard, K. A.; Kassem, M.; Kjems, J. *Mol Ther* **2010,** 18, (11), 2018-27.
31. Wagner, D. E.; Bhaduri, S. B. *Tissue Eng Part B Rev* **2012,** 18, (1), 1-14.
32. Kesharwani, P.; Gajbhiye, V.; Jain, N. K. *Biomaterials* **2012,** 33, (29), 7138-50.
33. Howard, K. A.; Rahbek, U. L.; Liu, X. D.; Damgaard, C. K.; Glud, S. Z.; Andersen, M. O.; Hovgaard, M. B.; Schmitz, A.; Nyengaard, J. R.; Besenbacher, F.; Kjems, J. *Molecular Therapy* **2006,** 14, (4), 476-484.
34. Xu, Q. X.; Leong, J. Y.; Chua, Q. Y.; Chi, Y. T.; Chow, P. K. H.; Pack, D. W.; Wang, C. H. *Biomaterials* **2013,** 34, (21), 5149-5162.
35. Andersen, M. O.; Howard, K. A.; Paludan, S. R.; Besenbacher, F.; Kjems, J. *Biomaterials* **2008,** 29, (4), 506-12.
36. Gao, S.; Hein, S.; Dagnæs-Hansen, F.; Weyer, K.; Yang, C.; Nielsen, R.; Christensen, E. I.; Fenton, R. A.; Kjems, J. *Theranostics* **2014**, 4, (10), 1039-51.
37. Ballarín-González, B.; Dagnaes-Hansen, F.; Fenton, R. A.; Gao, S.; Hein, S.; Dong, M.; Kjems, J.; Howard, K. A. *Mol Ther Nucleic Acids* **2013**, 2, e76.
38. Hirsh, V. *Clin Lung Cancer* **2009,** 10, (4), 223-9.
39. Yang, T. M.; Barbone, D.; Fennell, D. A.; Broaddus, V. C. *Am J Respir Cell Mol Biol* **2009,** 41, (1), 14-23.
40. Li, B.; Jiang, B.; Boyce, B. M.; Lindsey, B. A. *Biomaterials* **2009,** 30, (13), 2552-8.
41. Li, B.; Jiang, B.; Dietz, M. J.; Smith, E. S.; Clovis, N. B.; Rao, K. M. *J Orthop Res* **2010,** 28, (1), 48-54.
42. Shah, N. J.; Hyder, M. N.; Moskowitz, J. S.; Quadir, M. A.; Morton, S. W.; Seeherman, H. J.; Padera, R. F.; Spector, M.; Hammond, P. T. *Sci Transl Med* **2013,** 5, (191), 191ra83.
43. Jayant, R. D.; McShane, M. J.; Srivastava, R. *Int J Pharmaceut* **2011,** 403, (1-2), 268-275.
44. Li, H.; Ogle, H.; Jiang, B.; Hagar, M.; Li, B. *J Orthop Res* **2010,** 28, (8), 992-9.
45. Laufer, G.; Kirkland, C.; Cain, A. A.; Grunlan, J. C. *ACS Appl Mater Interfaces* **2012,** 4, (3), 1643-9.
46. Zheng, Z.; Yin, W.; Zara, J. N.; Li, W.; Kwak, J.; Mamidi, R.; Lee, M.; Siu, R. K.; Ngo, R.; Wang, J.; Carpenter, D.; Zhang, X.; Wu, B.; Ting, K.; Soo, C. *Biomaterials* **2010,** 31, (35), 9293-300.

47. Stevanovic, M.; Uskokovic, V.; Filipovic, M.; Skapin, S. D.; Uskokovic, D. *ACS Appl Mater Interfaces* **2013,** 5, (18), 9034-42.
48. Shen, K. T.; Chen, M. H.; Chan, H. Y.; Jeng, J. H.; Wang, Y. J. *Food Chem Toxicol* **2009,** 47, (8), 1864-71.
49. Salva, E.; Kabasakal, L.; Eren, F.; Ozkan, N.; Cakalagaoglu, F.; Akbuga, J. *Nucleic Acid Ther* **2012,** 22, (1), 40-8.
50. Xu, Y.; Wen, Z.; Xu, Z. *Anticancer Res* **2009,** 29, (12), 5103-9.
51. Qi, L.; Xu, Z.; Jiang, X.; Li, Y.; Wang, M. *Bioorg Med Chem Lett* **2005,** 15, (5), 1397-9.
52. Dass, C. R.; Choong, P. F. M. *J Microencapsul* **2008,** 25, (4), 275-279.
53. Vinas-Castells, R.; Holladay, C.; di Luca, A.; Diaz, V. M.; Pandit, A. *Bioconjugate Chem* **2009,** 20, (12), 2262-2269.
54. Chen, M.; Gao, S.; Dong, M.; Song, J.; Yang, C.; Howard, K. A.; Kjems, J.; Besenbacher, F. *ACS Nano* **2012,** 6, (6), 4835-44.
55. Achille, C.; Sundaresh, S.; Chu, B.; Hadjiargyrou, M. *PLoS One* **2012,** 7, (12), e52356.

Figure Legends

Figure 1. The clinical problem we are addressing is shown in (a). When tumors metastasize to the bone they are resected surgically but often residual tumor cells are left behind causing cancer recurrence. A void filler, e.g. the scaffold used in this study (b), is implanted in the void to support the bone and by releasing cytotoxic drugs residual cancer cells may be killed. Subsequently, bone cells grow into the scaffold and regenerate the missing bone while the scaffold matrix is degraded. As part of this study we try to imitate the clinical scenario *in vitro* by looking at drug release from a scaffold to adjacent cancer cells (c).

Figure 2. Non-functionalized scaffolds (a, b) and chitosan/siRNA nanoparticle functionalized scaffolds (c, d) were visualized using SEM. Magnification was 200x (a, c) and 1000x (b, d).

Figure 3. Median GFP fluorescence in GFP expressing cancer cells grown 2 days together with non-functionalized scaffolds (NF) or scaffolds functionalized with chitosan nanoparticles containing mismatched control siRNA (siMM) or siRNA targeted to GFP (siGFP). ANOVA(H1299) p-value = 0.0002, ANOVA(HeLa) p-value = 0.07 and ANOVA(U251) p-value = 0.007. n = 3 except for HeLa /siMM) (n = 2) and non-functionalized scaffold/U251 (n = 1).

Figure 4. GFP silencing in GFP^+ H1299 cells. (a) Histograms over GFP fluorescence in cells grown for 3 days in the presence of scaffolds functionalized with chitosan nanoparticles containing siMM control siRNA (dark shading) or GFP targeted siRNA (light shading). (b) Median GFP fluorescence normalized to the no-scaffold control group (NS) for cells grown 3 (black bars) or 7 days (grey bars), the other groups are non-functionalized scaffolds (NF) and scaffolds functionalized with

chitosan nanoparticles containing mismatched siRNA (siMM) or GFP targeted siRNA (siGFP). ANOVA p-value = 5E-12, n = 3.

Figure 5. Median GFP fluorescence in GFP expressing H1299 lung cancer cells grown with or without DSRED expressing mMSCs in the presence of non-functionalized scaffolds (NF), scaffolds functionalized with chitosan nanoparticles containing mismatched (siMM) or GFP specific siRNA (siGFP). ANOVA p-value = 4E-9, n = 3.

Figure 6. Viability in cells grown for 3 days together with no scaffolds (NS), non-functionalized scaffolds (NF) or scaffolds functionalized with chitosan nanoparticles containing mismatched siRNA (siMM). ANOVA p-value = 1E-9, n = 3

Figure 7. Viability in H1299 lung cancer cells grown for 3 days together with non-functionalized scaffolds (RNA = No) or scaffolds functionalized with chitosan nanoparticles containing mismatched siRNA (RNA = siMM) or BCLw targeted siRNA (RNA = siBCLw). Some of the scaffolds were also functionalized with 0.909μg doxorubicin (Dox = Yes). ANOVA p-value = 8E-9, n = 4.

Figure 8. Release of Cy3-labeled siRNA from chitosan/siRNA nanoparticle functionalized scaffolds. (a) The cumulative release of Cy3-labeled siRNA from chitosan/Cy3-siRNA nanoparticle functionalized scaffolds as a percentage of theoretical total loading. (b-d) The fluorescence intensity of scaffolds with no siRNA (b), non-fluorescent siRNA (c) or Cy3-labeled siRNA (d) as seen in a fluorescence microscope. ANOVA p-value = 4E-5, n = 3.

Figure S1. Images of H1299 cells after being cultured for 48 hours without scaffolds (a), with scaffolds not loaded with chitosan/siRNA nanoparticles (b), with scaffolds loaded with chitosan nanoparticles formulated with control-siRNA nanoparticles (c) or with scaffolds loaded with doxorubicin and chitosan nanoparticles formulated with control-siRNA nanoparticles (d).

Figure S2. Images of hMSCs stained for alkaline phosphatase (red) after being cultured in maintenance or osteogenic medium for 7 days without scaffolds or with scaffolds coated with chitosan/siRNA with or without doxorubicin as indicated. Three replicas are shown.

a

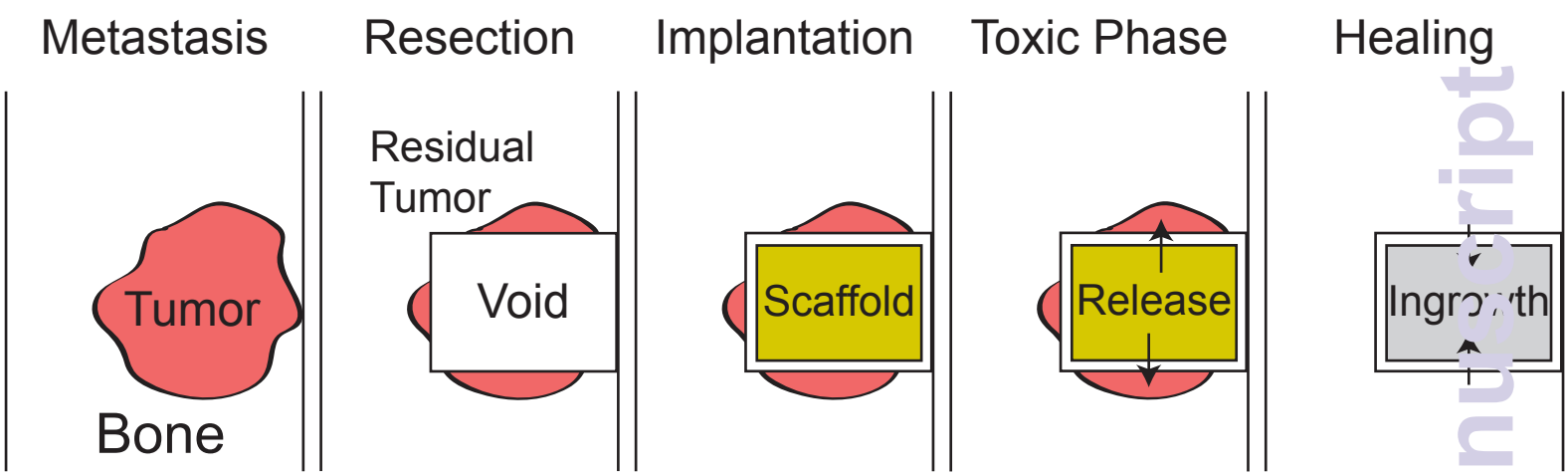

b

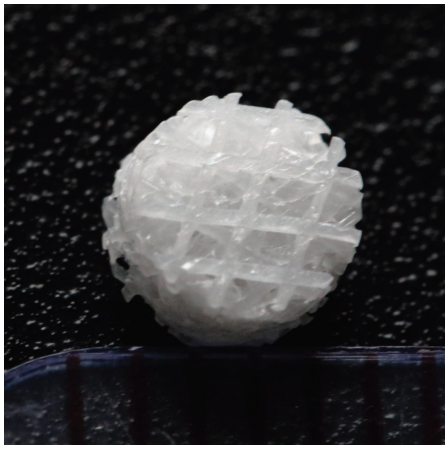

c

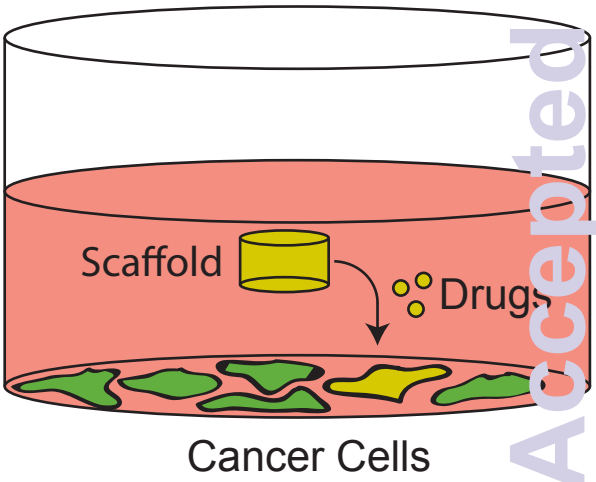

a

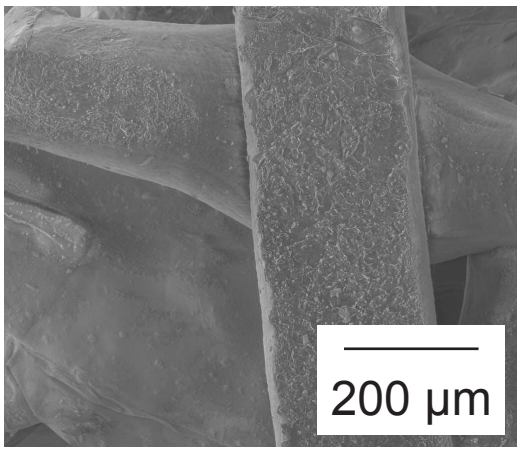

b

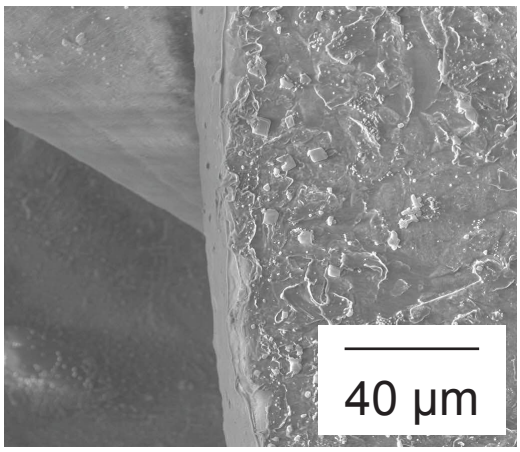

c

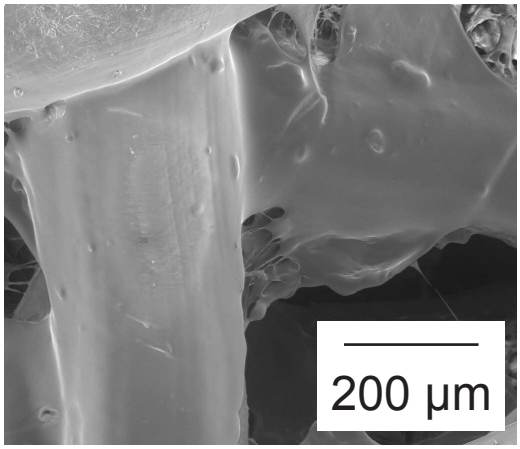

d

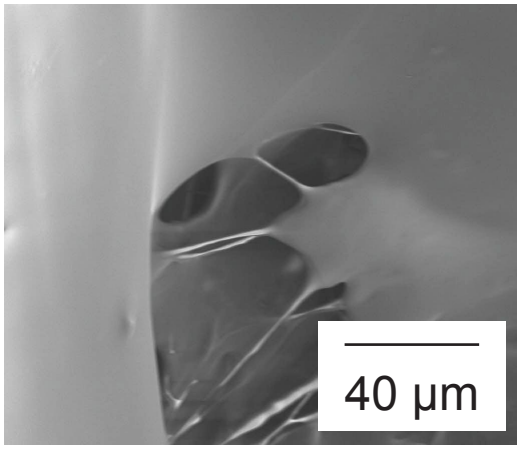

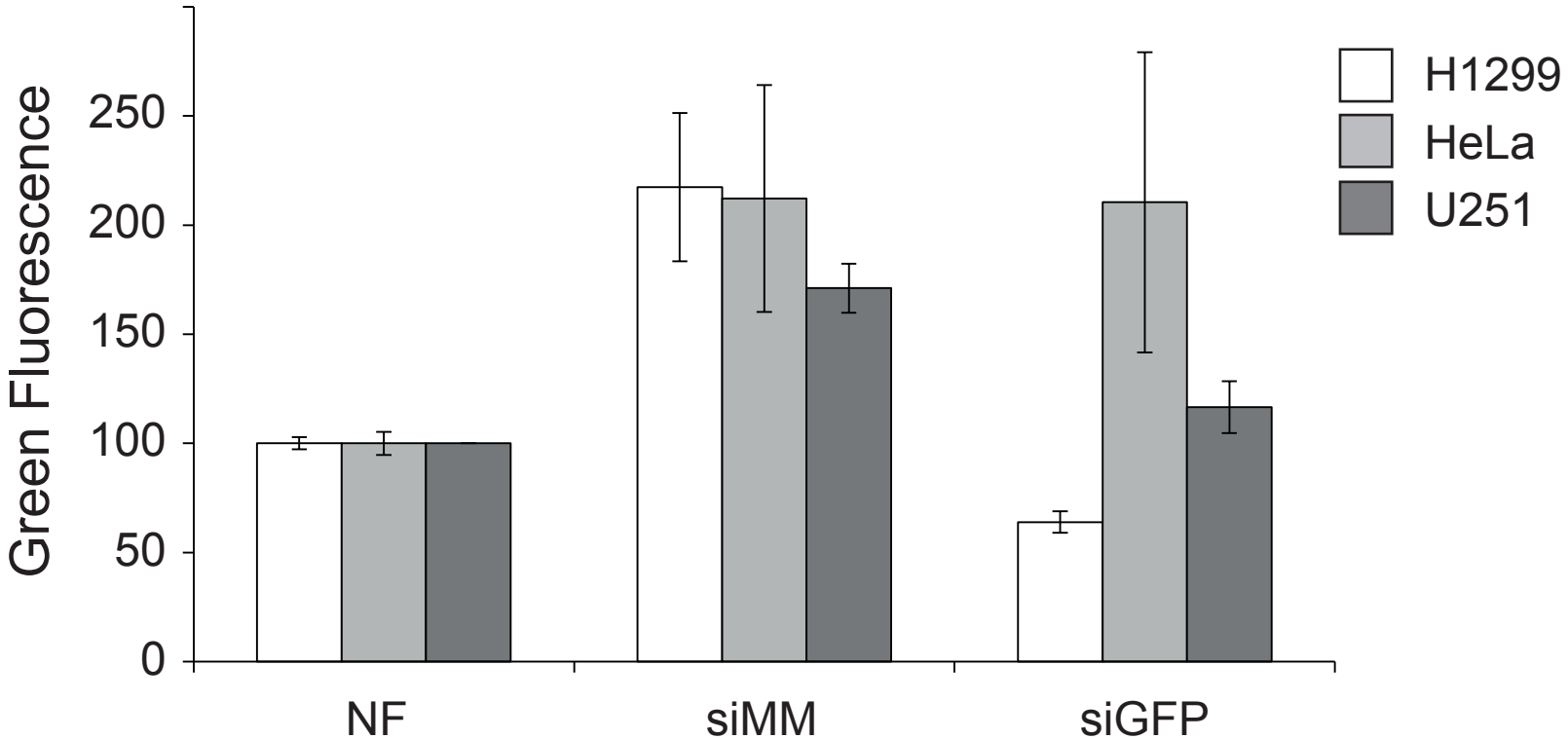

a

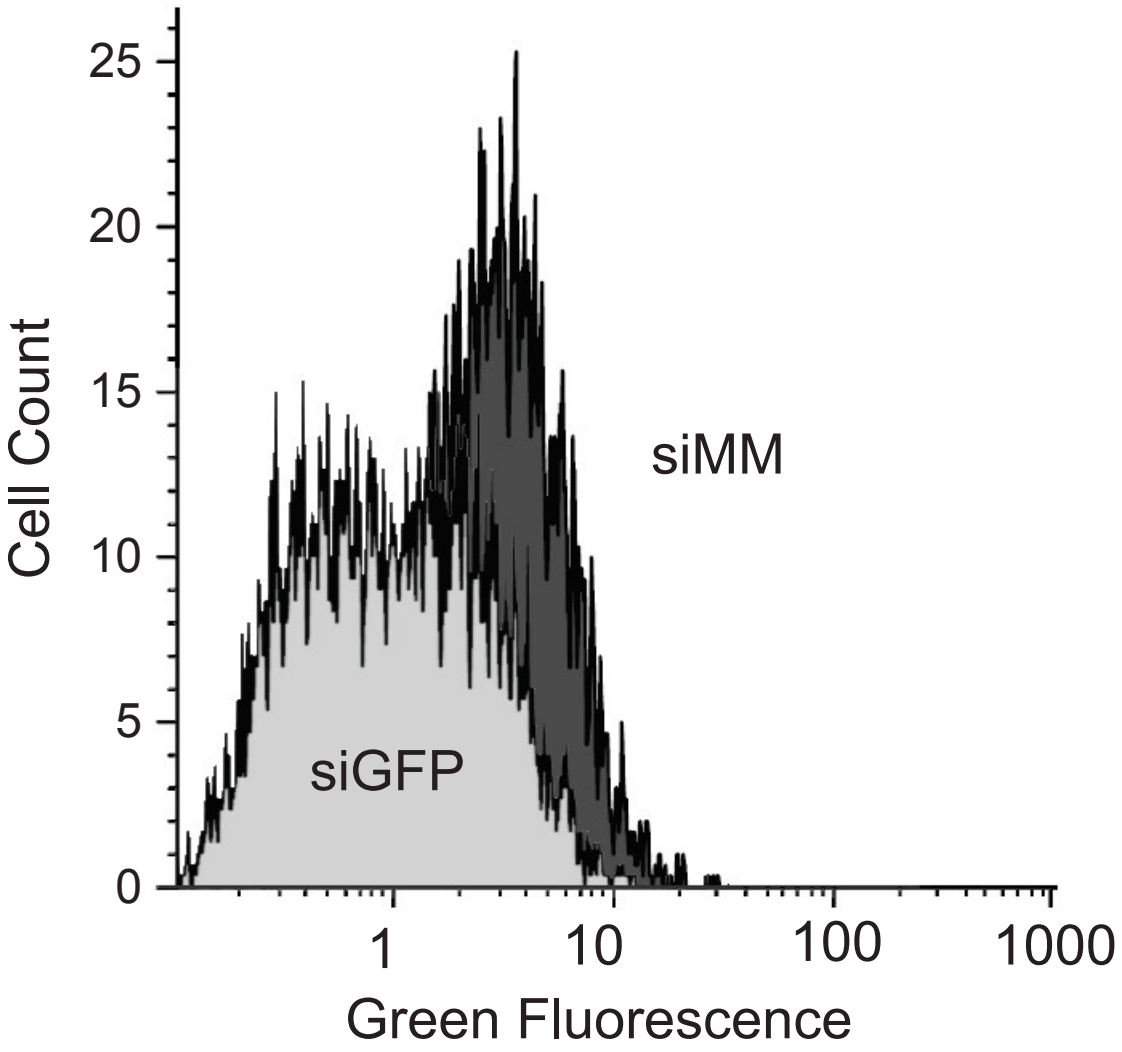

b

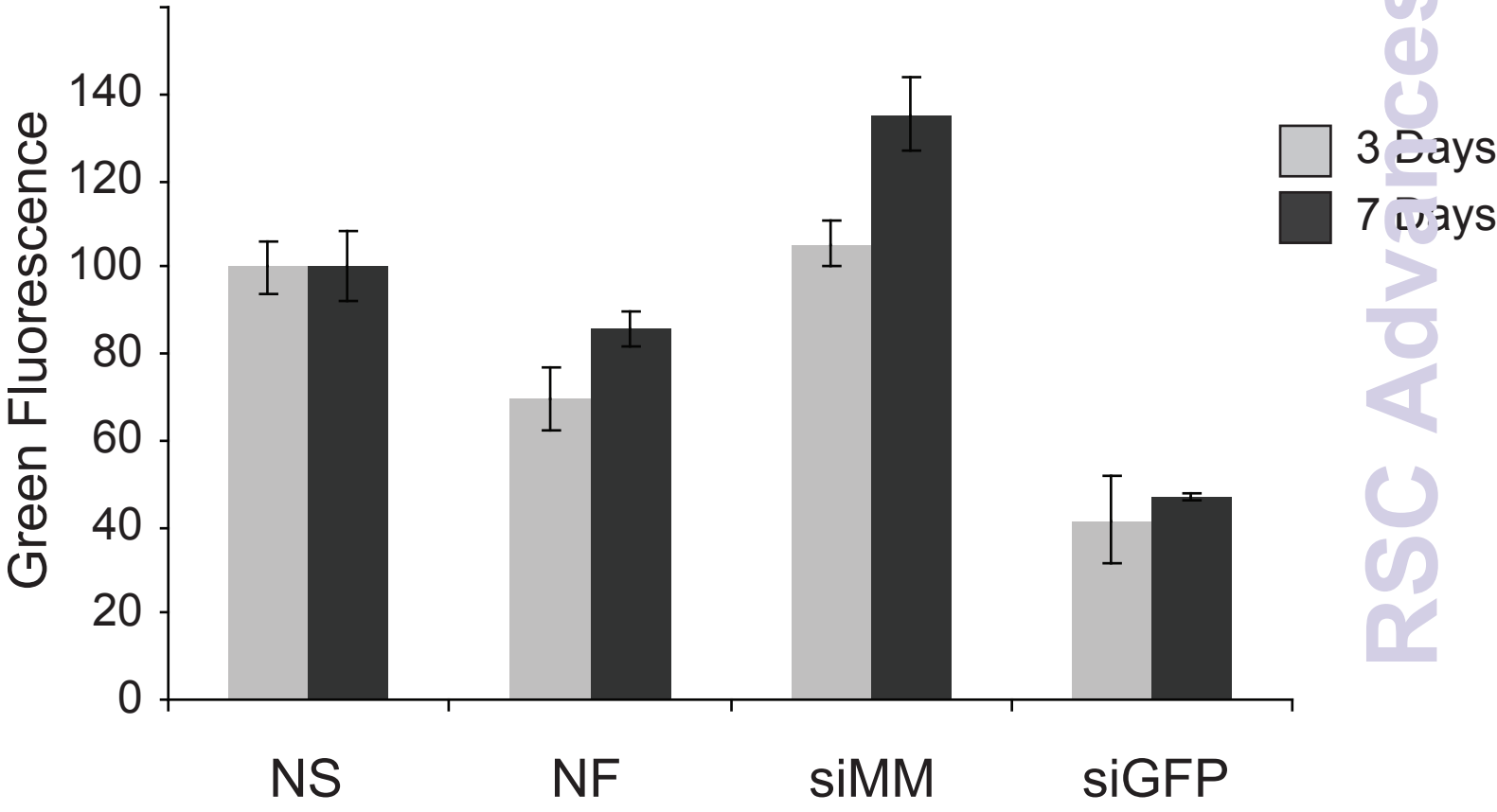

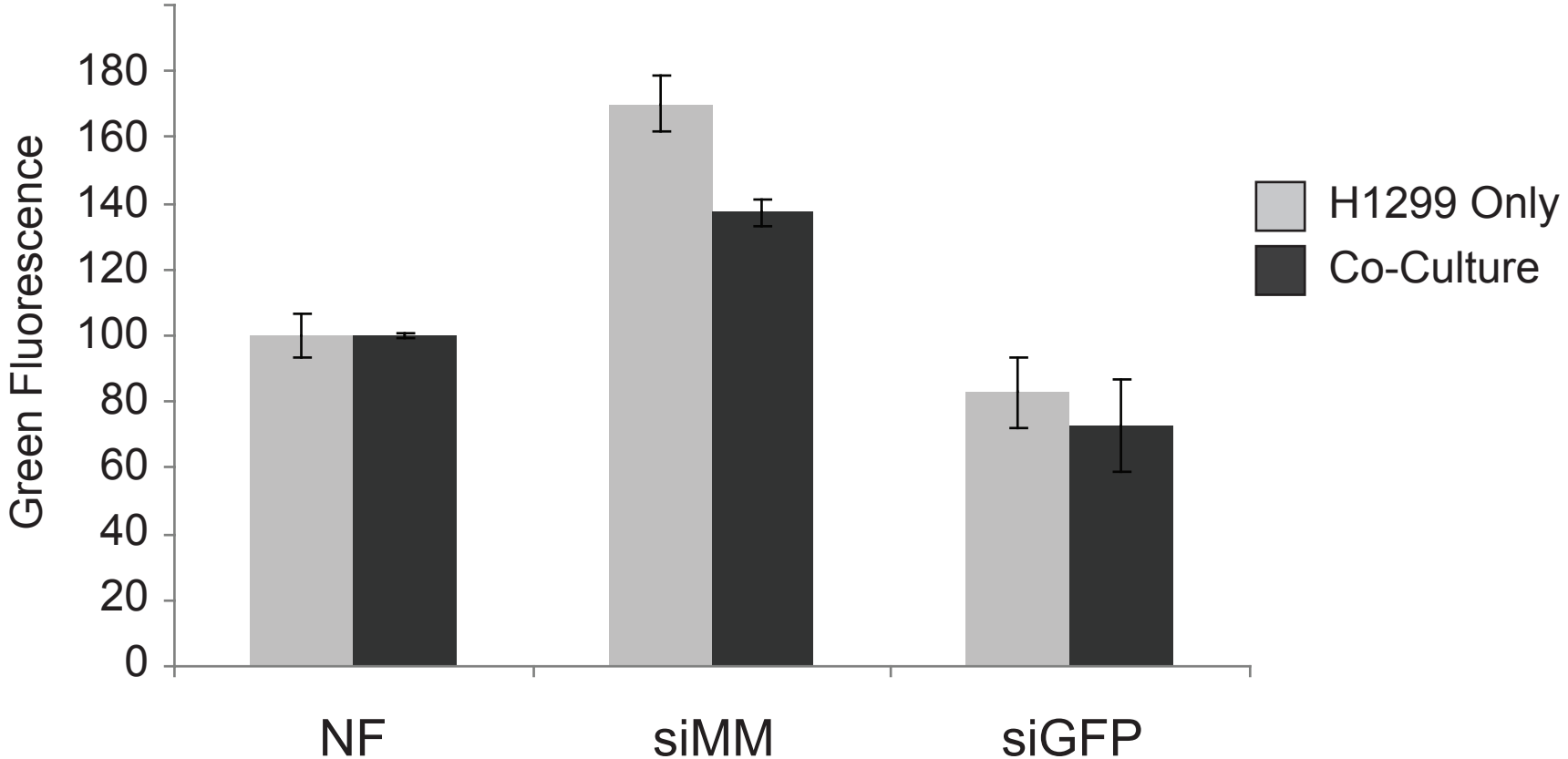

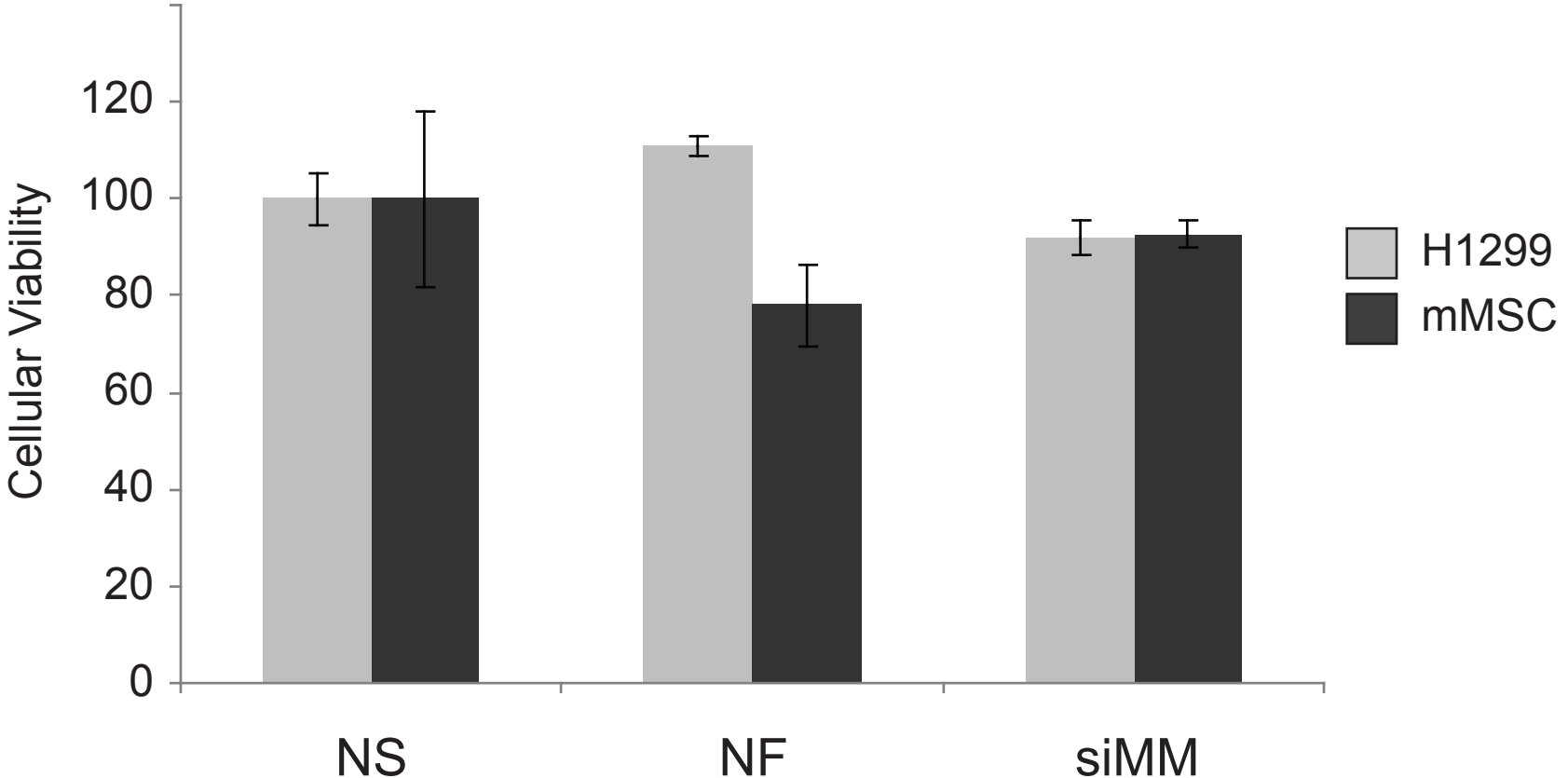

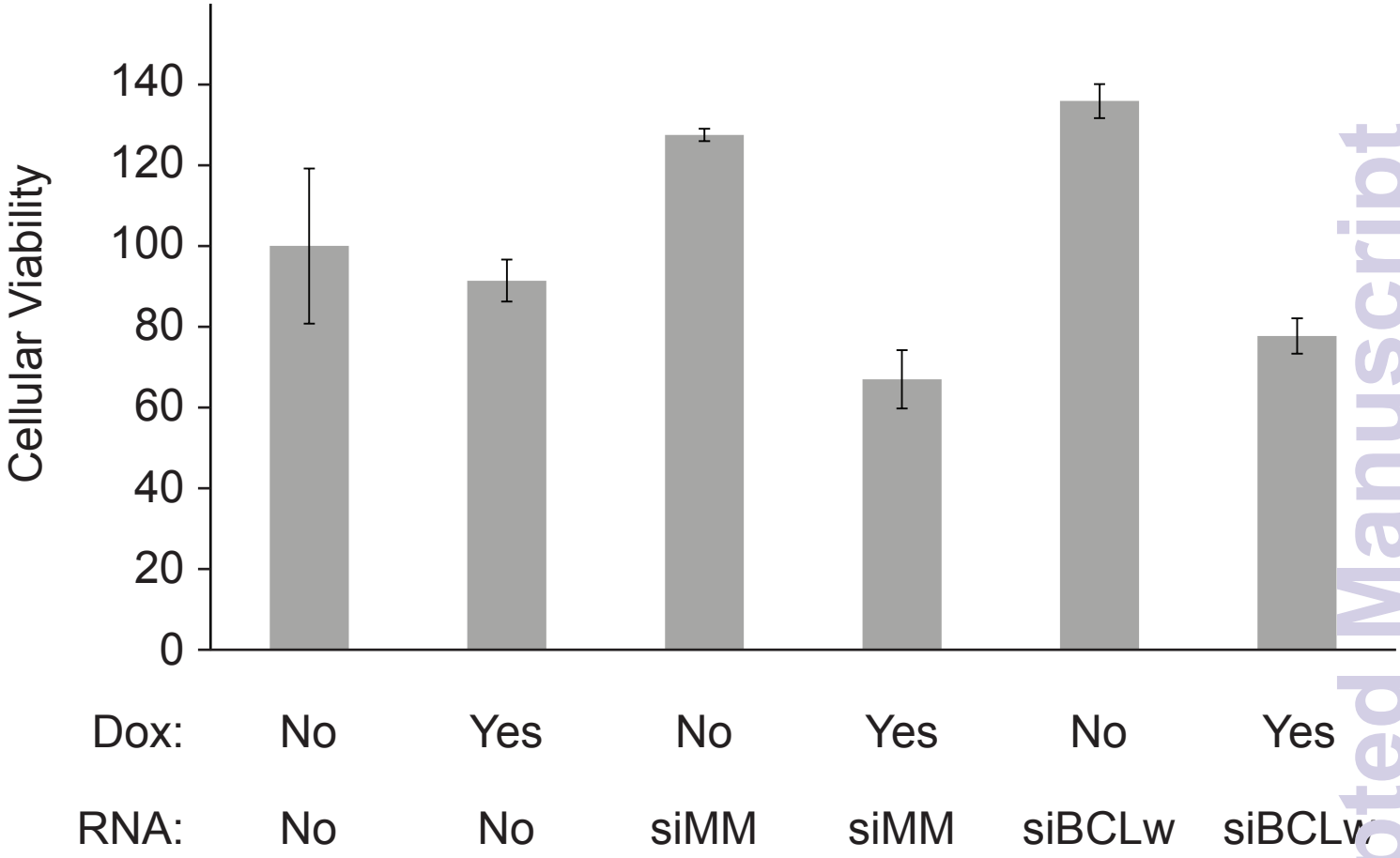

a

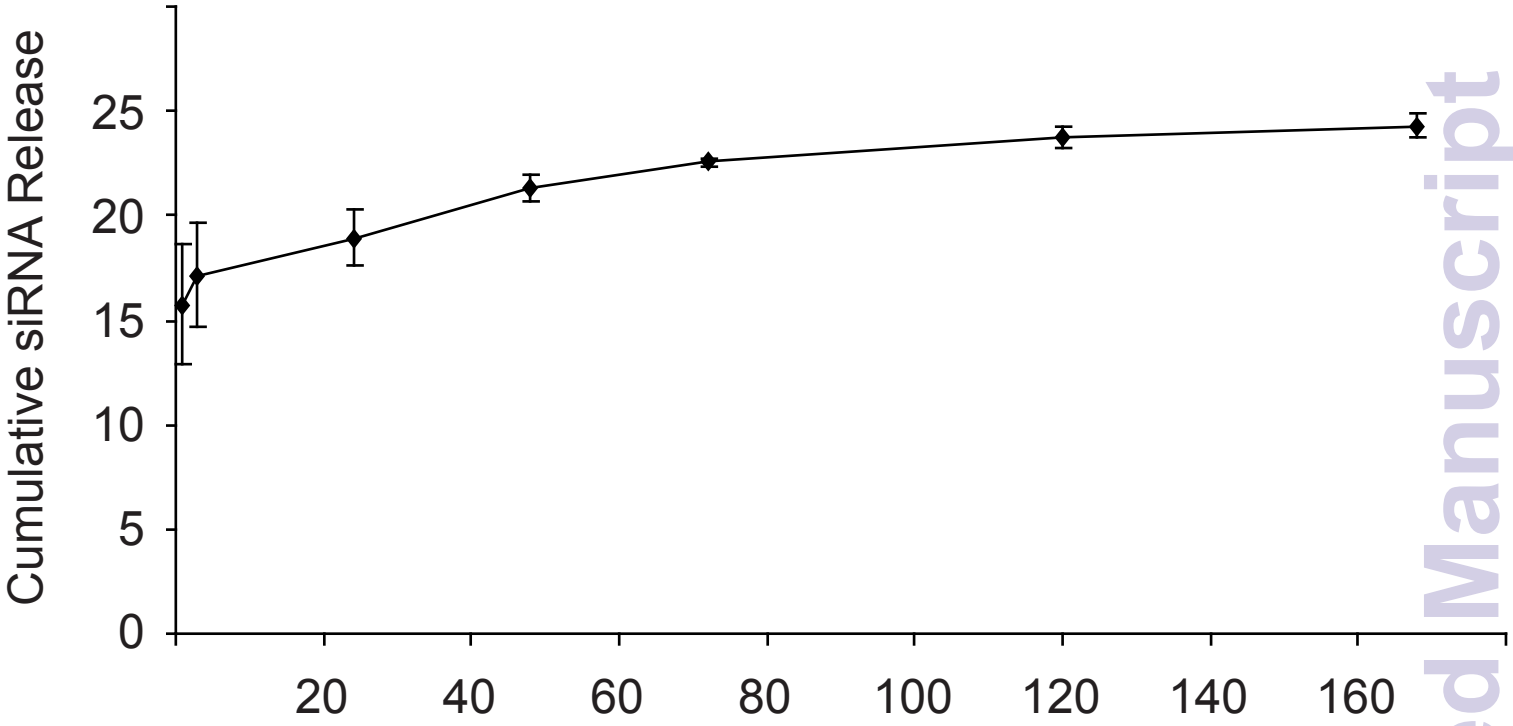

b

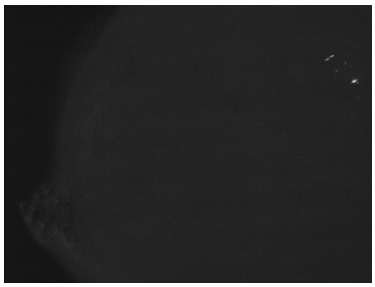

c

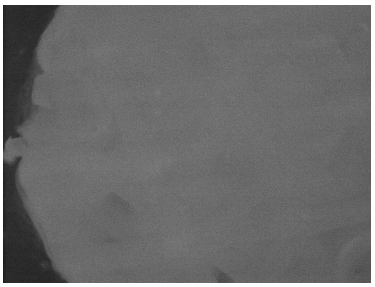

d